Replies to the Reviewers

Dear reviewers,

We are truly grateful to reviewers' critical comments and thoughtful suggestions. Based on these comments and suggestions, we have made careful modifications on the original manuscript. We are now sending the revised article. Please see our point to point responses to all comments below, and the corresponding revisions in the manuscript. In the revised manuscript, the biggest changes are mainly in the simulation system:

1) New instrument parameters of Aeolus were used according to ADM-Aeolus Algorithm Theoretical Basis Document (ATBD) Level1B products (Reitebuch et al., 2018)

2) The noise of detection unit was considered for that the impact of the noise cannot be negligible.

The comments and suggestions you gave are marked in blue, our modifications are marked in black, the original texts are marked in italic black, and our reasons for the modifications are marked in red. We hope the new manuscript will meet your magazine's standard. Below you will find our point-by-point responses to the reviewers' comments/ questions:

Reviewer 1:

General Comments

1. The presented results are interesting and potentially useful input for discussions on an Aeolus follow-on mission. The main question, which has not been answered in the paper is: why selecting orbits other than dawn-dusk, given that 3 satellites in a dawn-dusk orbit gives already quite good global coverage, without reducing wind quality due to increased solar background? See Fig.4 of Marseille et al (2008). Is there some indication that different local overpass times would be favorable for NWP? Please elaborate on this in the paper.

Response: The main purpose of this manuscript is to access the impact of solar background radiation (SBR) on the accuracy of wind observations for spaceborne Doppler wind lidar (DWL). For spaceborne DWLs operate on sun-synchronous orbits, the dawn-dusk orbit will receive minimum SBR, and the noon orbit will receive maximum SBR. The spaceborne DWLs operate on the sun-synchronous orbits with local time of ascending node (LTAN) crossing of 15:00 will receive medium SBR.

In this paper, the impact of different local overpass times on NWP was not taken into account. The selection of the three orbits was based on the following three aspects:

(1) The solar background radiation received by these three orbits is representative for sun-synchronous orbits.

(2) The observation coverage would be improved with three Aeolus-type spaceborne DWLs operating on the 3 orbits with LTAN crossing of 18:00, 15:00, and 12:00.

(3) We could reconstruct wind diurnal cycle with joint observations of the three spaceborne DWLs.

Based on the three above aspects, paragraph 2 of Introduction was modified:

Original: Page 2, ln. 43

The future spaceborne DWLs may operate on different orbits which should be related to their observation purposes. Aeolus operates on the sun-synchronous, dawn-dusk orbit to minimize the impact of solar background radiation (SBR) on the accuracy of wind observations (Heliere et al., 2002, Baars et al., 2019). The SBR is defined as the top-of-atmosphere (TOA) radiance which directs to the telescopes of spaceborne DWLs, and the solar background noise (SBN) is the photon counts excited by SBR and imaged on the photon detectors (Zhang et al., 2018) which would lower the observation accuracy by Poisson noise (Liu et al., 2006, Hasinoff et al., 2010). The dawn-dusk orbit is an optimal proposal to lower SBR for spaceborne DWLs operating on sun-synchronous orbits. If the future spaceborne DWLs would operate on the sun-synchronous orbits with different local time of ascending node (LTAN) crossing, the received SBR would become larger which would lead to higher uncertainties of wind observations.

Modified:

Aeolus operates on the sun-synchronous, dawn-dusk orbit to minimize the impact of solar background radiation (SBR) on the accuracy of wind observations (Heliere *et al.*, 2002, Baars *et al.*, 2019). The SBR is defined as the top-of-atmosphere (TOA) radiance which directs to the telescopes of spaceborne DWLs, and the solar background noise (SBN) is the photon counts excited by SBR and imaged on the photon detectors (Zhang *et al.*, 2018) which would lower the observation accuracy by Poisson noise (Liu *et al.*, 2006, Hasinoff *et al.*, 2010). The dawn-dusk orbit is an optimal proposal to lower SBR for spaceborne DWLs operating on sun-synchronous orbits. The future spaceborne DWLs may operate on different orbits which should be related to their observation purposes. For example, according to Marseille et al. (2008), larger coverage of wind observations would perform better in improving results of NWP. Furthermore, if the wind field at about 00:00/12:00 or 03:00/15:00 can be observed, we can reconstruct the wind speed diurnal cycle combing with the wind observations of Aeolus. If the future spaceborne DWLs would operate on the sun-synchronous orbits with different local time of ascending node (LTAN) crossing, the received SBR would become larger which would lead to higher uncertainties of wind observations.

2. In connection to this. Line 43: "The future spaceborne DWLs may operate on different orbits which should be related to their observation purposes". Which observation purposes are related to 12:00 or 15:00 local overpass times? See also line 72: "Assuming the future Aeolus-type spaceborne DWLs will operate on the sun-synchronous orbits with different LTAN". Based on what assumption?

Response: With joint observations of the three Aeolus-type spaceborne DWLs, we could reconstruct the wind diurnal cycle as mentioned in comment 1.

3. The realism of the simulations can be largely improved by comparing Aeolus measured SBR with simulated Aeolus SBR. Information on Aeolus measured SBR and the impact on Aeolus wind quality is found in the attached supplementary material. Based on this information, the authors can test the realism of their simulations.

Response: Thanks very much for providing the material to verify the realism of the simulations.

1) We cannot simulate the measured SBR with our model for that the duration times for background measurements are variable. The highest duration times are 3750 μs, while the lowest duration times are 2.1 μs. To simulate the measured SBR with one-year range, the corresponding duration times for background measurements are needed which may be contained in the L1A data. However, the L1A data are not openly accessible.

2) The solar background noise (SBN) received by Aeolus is determined by the geometry of solar and satellite, atmospheric conditions, and earth reflectance. And the solar zenith angle (SZA) of the off-nadir points is the main determinants. The simulated SZAs of the off-nadir points within one-year range are shown in Fig. 1. When the SZA is greater than 90 degrees as the horizontal red line shows, the received SBR could be negligible. Comparisons between Fig. 1 (a, b) show high consistence. Both of them are periodic. The values of them reach maximum near summer solstice and reach maximal near winter solstice. And the values of SBR reach minimal values near spring and autumn equinox. The 4 time ranges in Fig. 1 (a) divided by 8 red lines denote 15 days near autumn equinox, winter solstice, spring equinox, summer solstice.

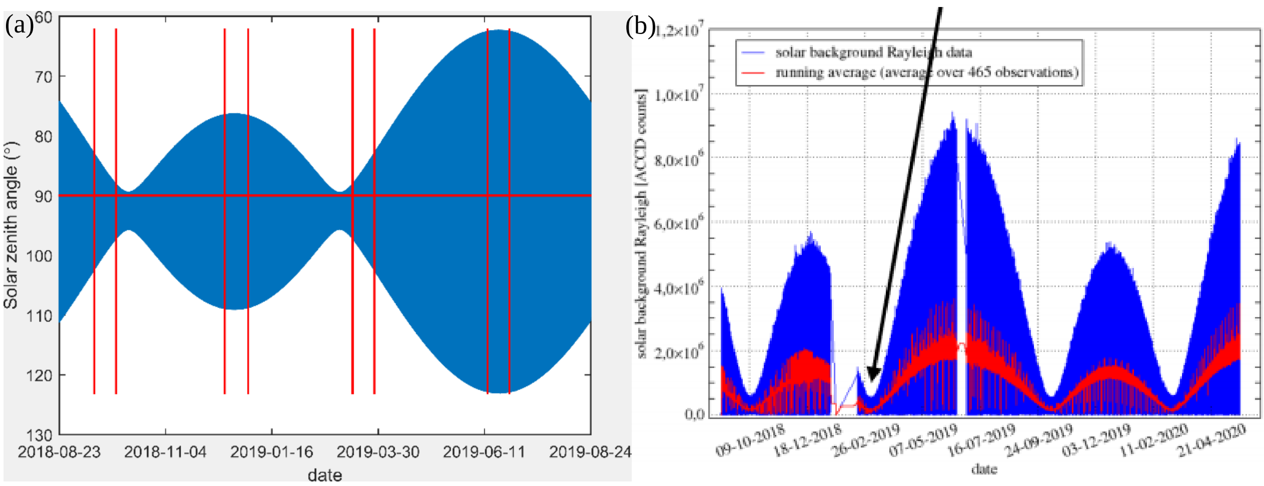

Fig. 1. (a) The simulated solar zenith angle of the off-nadir points of Aeolus within one-year range.

(b) Orbital variation of Rayleigh solar background noise (obtained from supplement).

3) The received SBR within 15 days near summer and winter solstice was simulated. And the SBR in summer and winter solstice was converted to ACCD counts of Rayleigh channel as is illustrated in Fig. 2. As Fig. 2 illustrated, the amount of ACCD counts near summer and winter solstice are consistent with Fig. 1 of the supplement. And SBN excited on Rayleigh channel are periodic as the subgraph of the supplement shows.

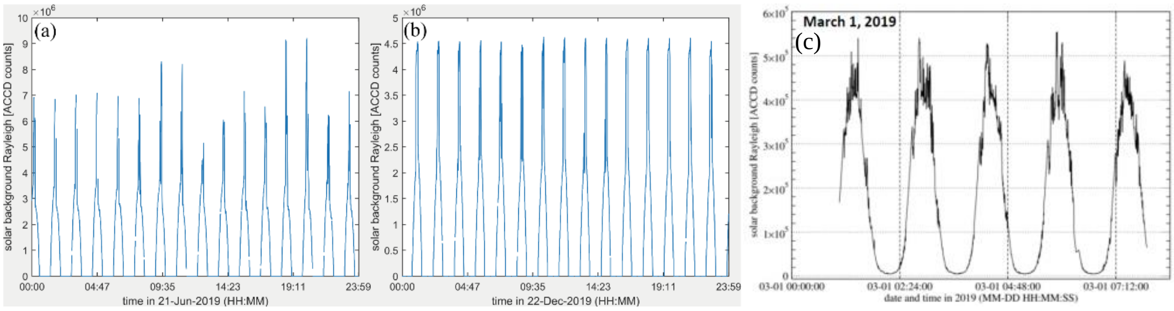

Fig. 2. The received SBN of Rayleigh channel (A+B) within 1 day. (a) simulated SBN near summer solstice, (b) simulated SBN near winter solstice, (c) measured SBN.

4) Assuming under the same atmospheric conditions, how much difference will the wind observations uncertainties obtained by using the new and old parameters be? The simulated uncertainties of wind observations under cloud-free atmospheric condition are illustrated in Fig. 3. The corresponding SZA of Fig. 3 is 70°, and the related SBR is 72.19 $mW \cdot m^{-2} \cdot sr^{-1} \cdot nm^{-1}$. As Fig. 3 (a) shows, the difference of uncertainties simulated using old and new parameters is large. The largest and average difference is 2.17 and 0.61 m/s, respectively. Fig. 3 (b) illustrated that the SNR simulated using new parameters is obviously large than the results using old parameters. The combination of Figs. 3 (c, d) can account this phenomenon. In Fig. 3 (c), the simulated useful signal of Rayleigh channel is relatively close, almost no difference. However, Fig. 3 (d) illustrated that the simulated SBN obtained using old parameters is much large than that of new parameters. Why the SBN simulated using old parameters is much larger than that of new parameters? As Tab. 1 illustrated, under old parameters, the Free Spectral Range of Rayleigh channel and FWHM of the FP interferometers of the old parameters is much larger than that of the new parameters. And in the simulation process, the SBN is regarded as following uniform distribution. Wider transmission bandwidth of Rayleigh channel will lead to higher solar background energy, which would lower the SNR of Rayleigh channel, and then increase the uncertainties of wind observations.

Considering the difference in simulated wind observation uncertainties between the old and new parameters. In the modified manuscript, new instrument parameters were used.

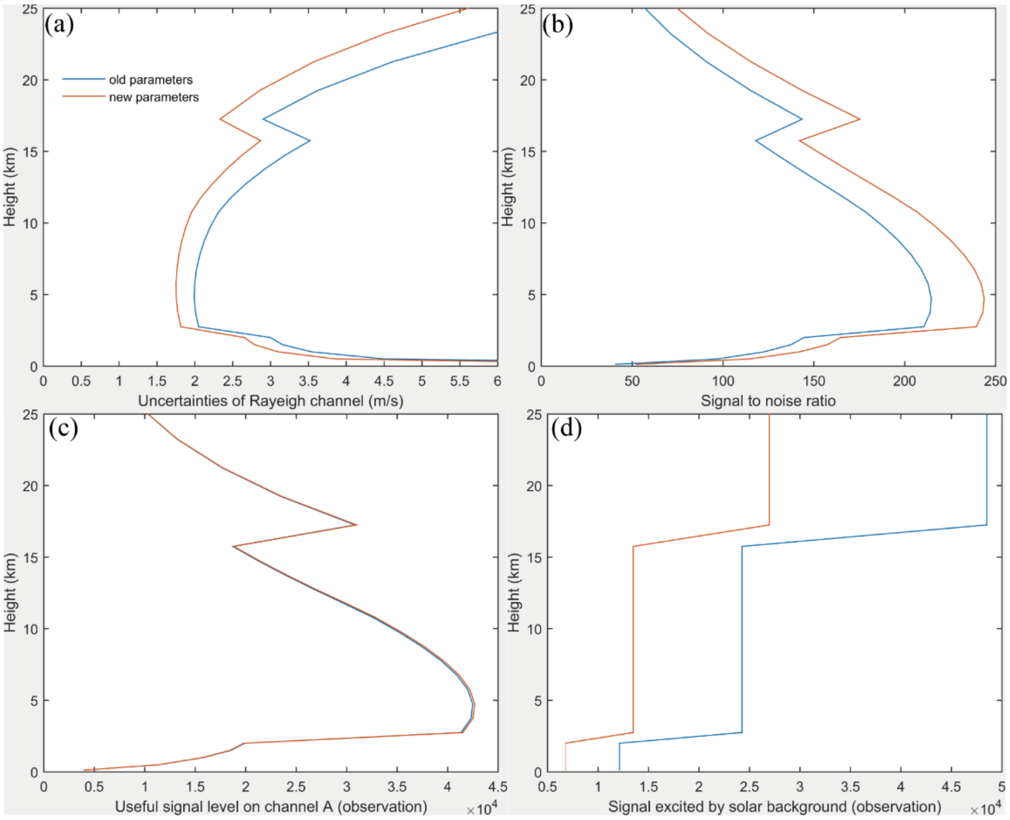

Fig.3. Some simulation results obtained using old and new instrument parameters. (a)wind observations uncertainties; (b)Signal to noise ratio; (c)Useful signal; (d)Signal excited by SBN.

5) To verify the correctness of our simulation model, we reconstructed Fig. 2 of the supplement using new parameters of Tab. 1 and the results are shown in Fig. 4. In the simulation, the typical and worst SBR are set as 72.50 and 156.00 mW·m^{-2}·sr^{-1}·nm^{-1}. The comparisons between Fig. 4 and Fig. 2 of the supplement show large difference. In Fig. 2 of the supplement, when the useful signal in channel A reach 5000, the related wind observation uncertainty is about 4 m/s. In our simulation, the uncertainty is about 8 m/s when the useful signal in channel A is about 5000. However, the uncertainties of wind observation are about 2~3 m/s when the SBR is about 72.19 mW·m^{-2}·sr^{-1}·nm^{-1}. The results are reasonable. In our simulation, the photon counts excited by typical and worst SBN in channel A are 1.34*10^4 and 2.92*10^4 respectively when the vertical height of the range gate is 1 km. In Fig. 4, the useful signal in channel A is general between 2*10^4 ~ 3*10^4.

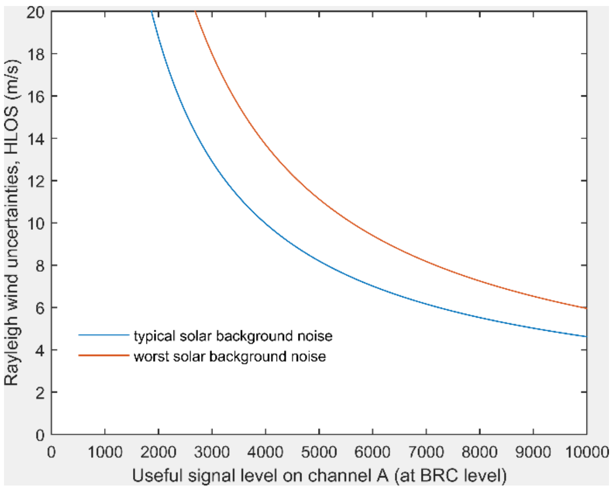

Fig. 4. The relationship between uncertainties of wind observations and useful signal of channel A on Rayleigh channel.

Minor Comments

4. line 60: "The received SBR of Aeolus ranges from 0 to 169 $mW \cdot m^{-2} \cdot sr^{-1} \cdot nm^{-1}$". That is worse than "On the two new orbits, the increments of averaged SBR received by the new spaceborne DWLs range from 39 to 56 $mW \cdot m^{-2} \cdot sr^{-1} \cdot nm^{-1}$" (line 14). Can the author please comment.

Response: Line 14: "On the two new orbits, the increments of averaged SBR received by the new spaceborne DWLs range from 39 to 56 $mW \cdot m^{-2} \cdot sr^{-1} \cdot nm^{-1}$." The sentence is referred to that the averaged SBR received by Aeolus-type instruments operate on the sun-synchronous orbits with LTANs of 15:00 and 12:00 is higher than that of Aeolus, and the average increment of SBR ranges from 39 to 56 $mW \cdot m^{-2} \cdot sr^{-1} \cdot nm^{-1}$. The conclusion is corresponding to the sentence: "Statistics illustrate that the averaged SBR of the three spaceborne DWLs are 20.99, 60.68, and 76.36 $mW \cdot m^{-2} \cdot sr^{-1} \cdot nm^{-1}$ respectively." (line 262). The sentence in line 14 may be ambiguous. In the revision, line 262 will be modified to make the sentence in line more clear as reviewer 2 suggest.

Modified:

Statistics illustrate that the averaged SBR of the three spaceborne DWLs are 20.99, 60.68, and 76.36 $mW \cdot m^{-2} \cdot sr^{-1} \cdot nm^{-1}$ respectively. The increments of averaged SBR received by the new spaceborne DWLs are 60.68-20.99=39.69 $mW \cdot m^{-2} \cdot sr^{-1} \cdot nm^{-1}$ and 76.36-20.99=55.37 $mW \cdot m^{-2} \cdot sr^{-1} \cdot nm^{-1}$.

5. Figure 1b is misleading since it suggests that all three Aeolus-type instruments operate during daytime at equal time intervals.

Response: Figure 1b illustrates the off-nadir points on earth surface of the three spaceborne DWLs operate on the sun-synchronous orbits with LTANs of 18:00, 15:00, and 12:00, respectively.

6. line 108: "Figure 1(b) shows that the solar zenith angle of the observation points of the two new Aeolus-type instruments is low compared to that of Aeolus". How can that be seen from the figure?

Response: In Figure 1 (b), the shaded area represents the night, the non-shaded area represents the day, and the dividing line between the shaded area and the nonshaded area is the dividing line between day and night. In Figure 1b, the trajectory of the off-nadir points of Aeolus is closer to the dividing line compared to the off-nadir points of Aeolus 2 and Aeolus 3. Therefore, it is supposed that the solar zenith angles of the off-nadir points of the two new orbits should be lower.

As the referee pointed, it is not clear to see the comparative relationship in the sun zenith angle of the three orbits. In the latter revision, we added a new figure to illustrate the fact in the revision (Fig. 2 of revised manuscript), as Fig. 8 shows, which illustrate the variations of SZA of the three orbits as time.

7. The simulations would be more useful if the operational Aeolus instrument would be used for reference 1. one measurement is composed of 20 accumulated shots onboard; 1 observation is obtained from averaging 30 measurements. 2. Assuming around 60mJ laser energy, which is consistent with current operational Aeolus laser-B 3. optical throughput is a factor 2-3 lower than expected. The authors can do simulations based on both this unexpected signal loss (worst case scenario) and without this loss, assuming that the problem can be identified and solved before the launch of the Aeolus follow-on mission (best case scenario). With the above settings 0% of Aeolus data would meet the mission requirement, rather than 88.01% as mentioned in Table 5. So, it would be interesting to extend Table 5, by presenting both best and worst case scenarios.

Response: In the manuscript, Aeolus was assumed to be operated on best case scenario. As is illustrated in Fig. 6, Aeolus performs better using new parameters. It is very meaningful if we can assess the impact of instrument operational instrument on the wind observation uncertainties combined with the operational Aeolus instrument. This is also a topic that I'm very interested in. I think it can be studied as the next topic when we could get access to Aeolus L1 measurement product.

8. line 118: "we focus on the simulation of the wind retrieved method on Rayleigh channel, and assume that the cross-talk effect between Mie channel and Rayleigh channel is negligible". Based on this assumption, you can remove mentioning over scattering ratio in section 3.1.

Response: Thanks for your kind mention. In the revision, we removed related expressions.

9. Derivation of Eq. (7) in Appendix could have been done more simple, by substituting A=B in Eq.(3) => $\sigma_{R_{ATM}} = \sigma_A/\left(N_A * sqrt(2)\right)$ Substituting Eq. (4) in Eq.(6) and setting A=B => $SNR_{Ray} = (N_A * sqrt(2))/\sigma_A$.

Response: Thanks for your kind suggestion. the method would make the derivation much more simple. In revisions, we simplified the derivation method according to your suggestions.

10. Figure 2. For the 15:00 and 12:00 UTC orbits, half the orbit is in full darkness (so no SBR contribution), the other half in full daylight (a large SBR contribution). How is this reflected in figure 2?

Response: In Fig. 2, the global distribution of maximum SBR in 1°×1° grid was illustrated.

When demonstrating the instrument parameters of spaceborne DWLs, people not only pay attention to the performance in general cases, but also in worst cases. Aeolus-type spaceborne DWLs would obtain maximum wind observation uncertainties with maximum SBR. For SBR, solar zenith angle is the dominant factor. The variations of solar zenith angles of the off-nadir points on the three orbits within one-year range are illustrated in Fig. 5 (Fig. 2 of modified manuscript), which indicates that received SBR would reach maximum values near summer solstice and reach maximal values near winter solstice.

As to the off-nadir points, the corresponding SBR would get maximum values near summer solstices in the north hemisphere, and the corresponding SBR would get maximum values near winter solstices in the south hemisphere. In order to study the performance of spaceborne DWLs in worst cases, we derived the SBR values of all off-nadir points in 15 days around summer and winter solstice, and divided the earth into 1°×1° grid, and picked the maximum SBR values in each grid out as the SBR in this grid, which would correspond to maximum Rayleigh wind observation uncertainties. In Fig. 2, the global distributions of maximum SBR in 1°×1° grid near summer and winter solstices in 15 days were plotted.

In original manuscript, the details of the method and data used to plot Fig. 2 were not clear. In the revision, the corresponding descriptions are added.

1) Ln 101, Para. 2 of subsection 2.1. We explained why the global distributions of maximum SBR near summer and winter solstices were derived in this manuscript.

Modified:

When demonstrating the instrument parameters of spaceborne DWLs, people also pay attention to the observation accuracy under worst cases. Solar zenith angle is the dominant factor for SBR received by spaceborne DWL. The variations of solar zenith angles of the off-nadir points on the three orbits within one-year range are illustrated in Fig. 2, which indicates that received SBR would reach maximum values near summer solstice and reach maximal values near winter solstice. For the off-nadir points in the north hemisphere, SBR will reach maximum near summer solstice. And SBR will reach maximum near winter solstice for the off-nadir points in the south hemisphere. In this paper, the global distributions of maximum SBR in 1°×1° grid near the summer solstice which range from June 14 to 28 and near the winter solstice which ranges from December 15 to 30 are used for the investigations of the worst cases with maximum Rayleigh channel wind observation uncertainties due to SBR. Furthermore, the annual variation characteristics of solar zenith angles are less obvious on the two new orbits compared to that of Aeolus as shown in Fig. 2, which indicates that the observations of two new spaceborne DWLs would more likely to suffer worst cases on Rayleigh channel compared to that of Aeolus.

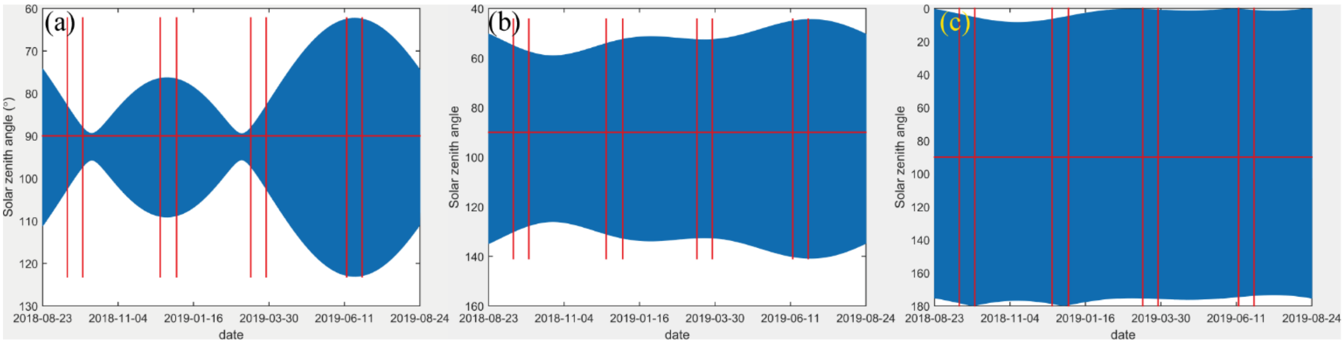

Fig. 5. The variations of solar zenith angles of the off-nadir points on the three orbits within one-year range. The 4 time ranges in Fig. 3 divided by 8 red lines denote 15 days near autumn equinox, winter solstice, spring equinox and summer solstice respectively.. Sun-synchronous orbit with Local Time of Ascending Nodes crossing (LTANs) of 18:00 (a), 15:00(b) and 12:00(c).

2) Ln 137, Para. 2, subsection 2.2. The method to derive the global distributions of maximum SBR was also added.

Original:

Then the SBR of off-nadir points was generated by radiative transfer model (RTM) libRadtran with the input of temperature, pressure, aerosol optical properties, and surface albedo (Emde et al., 2016). Once the atmospheric conditions and SBR were input to the simulation system, the HLOS winds and their corresponding uncertainties could be figured out.

Modified:

Then the SBR of off-nadir point was generated by radiative transfer model (RTM) libRadtran with the input of atmospheric optical properties, and surface albedo (Emde et al., 2016). Finally, the earth was divided into 1°×1° grid, and the maximum SBR in each grid is picked out as the worst cases of Rayleigh channel wind observation uncertainties due to SBR. Once the atmospheric conditions and SBR were input to the simulation system, the HLOS winds and their corresponding uncertainties in the grids could be figured out.

11. Also in Figure 3, I would expect bi-modal accuracy statistics with very good quality at the dark part of the orbit (no SBR) and low quality in the day-light part (high SBR). So, what is exactly displayed in Figure 3? Please present both statistics separately. In the caption of figure 3, mention that this is winds from the Rayleigh channel in clean air conditions.

Response (1): In Fig. 3 (Fig. 5 of the revised manuscript), the global distributions of SBR were averaged in 10° latitude. Atmospheric conditions of in 10° latitude average were obtained from Ozone Monitoring Instrument (OMI) database as mentioned in subsection 2.2 of the manuscript. Finally, the atmospheric conditions and SBR were input to spaceborne DWL simulation system, and 18 profiles of wind observation uncertainties were derived and plotted in Fig. 3 of original manuscript.

In order to explain what is displayed in Fig. 3 clearly, the original manuscript was modified.

Original: ln. 270 P10

Assuming the instrument parameters of the two new spaceborne DWLs were set to be the same as those of Aeolus, the profiles of wind observation uncertainties were derived as is shown in Fig. 3, which was obtained from the spaceborne DWLs simulation system using the 10 °latitude-averaged SBR shown in Fig. 2, for whose contour lines illustrated that the distributions of SBR were nearly horizontal to latitude. Each subgraph in Fig. 3 was obtained based on 18 wind uncertainty profiles.

Modified:

Based on the global distributions of maximum SBR of the three orbits illustrated in Fig. 3, the worst cases of Rayleigh channel with maximum wind observation uncertainties due to SBR were also derived as shown in Fig. 5. Considering that the distributions of maximum SBR were nearly horizontal to latitude, and to simplify the calculation, Fig. 5 was obtained using the 10 ° latitude-averaged SBR and atmospheric conditions.

Response (2): In the revised manuscript, the global distributions of wind observation uncertainties without the impact of SBR are added as Fig. 4 in the revision. At the dark part of the orbit, Rayleigh channel wind observation uncertainties are only influenced by atmospheric conditions, orbit selection has no impact on the wind observation without consideration of SBR. Therefore, in the revised manuscript, the global distributions of wind observation uncertainties without the impact of SBR in summer and winter are illustrated.

Response (3): The caption of Fig. 3 (Fig. 5 of revised manuscript) is revised.

Original:

Figure 3. The zonal distributions of wind uncertainty observed by the three spaceborne DWLs operated on the three orbits of which the instrument parameters are the same as those of Aeolus.

Modified:

Figure 5. The zonal distributions of Rayleigh channel wind uncertainties in clear air conditions observed by the three spaceborne DWLs operated on the three orbits of which the instrument parameters are the same as those of Aeolus.

Reviewer 2:

General Comments

1. The authors should compare SBR computed by means of their model with measured in-orbit SBR data for certain time ranges. The reviewer 1 provided some data in his review supplement. This would increase the confidence in the authors model. Moreover, plots over a year show that SBR measured by Aeolus is maximum in June and December (see again supplement). Thus the authors can argue that their investigations for June and December are for the worst cases with maximum Rayleigh channel wind errors due to SBR.

Response: Thanks for your suggestions. As to the comparison between simulated and measured SBR, we explained the topic in detail in the reply to Q3 of Reviewer 1. The main ideas are described briefly as follows:

First, because the solar background radiation is mainly determined by solar zenith angle of the off-nadir points, we computed the solar zenith angles of off-nadir points within one-year range. The variations of solar zenith angles are in consistent with the variations of in-orbit measured SBR indicate that the variation trend of simulated SBR would be in consistent with the measured SBR.

Then, we simulated SBR received by Aeolus during 15 days near summer and winter solstices. And the simulated SBR in the two days of summer and winter solstices was shown in Fig. 4 of the reply to reviewer 1 to compare with Fig. 1(a) of the supplement. The comparisons show that the two are consistent in variation trend and magnitude, which increase the confidence of our model.

In addition, in the ATBD L1B Products (issue 4.4 20.04.2018), the highest background integration times is 3750 μs which is related to 446 km vertical height of 25th range gate. In our simulation, the integration times for solar background radiation is 1680 μs which is related to 200 km vertical height of 25th range gate.

Furthermore, thanks very much for your suggestions, we have stated in the response to reviewer 1 that we are considering the worst conditions of solar background radiation in the manuscript and made corresponding changes in the manuscript.

2. In lines 60-61, the authors write that the "received SBR of Aeolus ranges from 0 to 169 mW*m^{-2}*sr^{-1}*nm^{-1}". The authors should give the corresponding reference. Aeolus measures primarily ACCD counts of SBR.

Response: Thanks for your kind reminder. The results were obtained from Zhang et al. (2019). We will add the citation in the revision.

Original:

The received SBR of Aeolus ranges from 0 to 169 $mW{\cdot}m^{-2}{\cdot}sr^{-1}{\cdot}nm^{-1}$. *Zhang et al., (2019) shows that the mean uncertainties in the wind observation of Aeolus would increase by 0.18, 0.69 m/s in the troposphere and stratosphere* *respectively as 20 mW·m^{-2}·sr^{-1}·nm^{-1} of SBR increases. When the SBR is greater than 80 mW·m^{-2}·sr^{-1}·nm^{-1}, the whole profiles of wind observations would be less accurate.*

Modified:

The study of Zhang et al., (2019) illustrates that the received SBR of Aeolus ranges from 0 to 169 mW·m^{-2}·sr^{-1}·nm^{-1}. And when the SBR is greater than 80 mW·m^{-2}·sr^{-1}·nm^{-1}, the whole profiles of wind observations would be less accurate.

3. It is of course possible and interesting to consider sun-synchronous orbits other than dawn-dusk orbits. The authors should explain their choice of orbits with LTANs of 15:00 and 12:00 in Section 2.1.

Response: Thanks for your reminder. In para. 1 of Section 2, we explained the choice of orbits with LTANs of 15:00 and 12:00. In order to make readers more clear about the reasons for this choice, explanation has been added in the revised manuscript.

Original: ln. 89, Para. 1 of section 2

In general, for sun-synchronous orbits, the spaceborne DWL runs on the dawn-dusk orbit would receive minimum SBR, and the spaceborne DWL runs on the noon-midnight orbit would receive maximum SBR. In order to study the impact of orbit selection on the wind observation accuracy, the spaceborne DWL runs on three sun-synchronous orbits with LTANs of 18:00, 15:00, and 12:00 respectively were proposed.

Modified:

In general, for sun-synchronous orbits, the spaceborne DWL runs on the dawn-dusk orbit (LTAN of 18:00) would receive minimum SBR, and the spaceborne DWL runs on the noon-midnight orbit (LTAN of 12:00) would receive maximum SBR. In order to study the impact of orbit selection on the wind observation accuracy, the spaceborne DWL runs on three sun-synchronous orbits with LTANs of 18:00, 15:00, and 12:00 respectively were proposed.

4. It becomes not clear which kinds of aerosols are considered by the authors in their simulations (only aerosols in the planetary boundary layer (PBL) or also above it). The authors should specify this. Furthermore, the authors should replace "clear sky" by "cloud-free" in lines 15 and 379 due to the presence of aerosols.

Response (1): In the manuscript, only the aerosols in the PBL were considered. The aerosol above it (stratospheric aerosols) were not taken into account. And the corresponding descriptions in Section 2.2 were modified.

Original: ln 131, para 2 of Section 2.2

and the lidar climatology of vertical aerosol structure for spaceborne lidar simulation studies (LIVAS) database (Amiridis et al., 2015), which was used to describe aerosol optical properties.

Modified:

and the lidar climatology of vertical aerosol structure for spaceborne lidar simulation studies (LIVAS) database (Amiridis *et al.*, 2015), which is used to describe aerosol optical properties, and only aerosols in the PBL are considered here.

Response (2): In the revision, we replaced "clear-sky" by "cloud-free" in lines 15 and 379.

Original: ln. 15

On the two new orbits, the increments of averaged SBR received by the new spaceborne DWLs range from 39 to 56 $mW{\cdot}m^{-2}{\cdot}sr^{-1}{\cdot}nm^{-1}$ *under clear skies*

Modified:

On the two new orbits, the increments of averaged SBR received by the new spaceborne DWLs range from 39 to 56 $\mathrm{mW{\cdot}m^{-2}{\cdot}sr^{-1}{\cdot}nm^{-1}}$ under cloud-free skies

Original: ln 379

The global distributions of SBR illustrate that the increments of averaged SBR range from 39 to 56 $mW{\cdot}m^{-2}{\cdot}sr^{-1}{\cdot}nm^{-1}$ *on the two new orbits compared to that of Aeolus under clear skies*

Modified:

The global distributions of SBR illustrate that the increments of averaged SBR range from 39 to 56 $\mathrm{mW{\cdot}m^{-2}{\cdot}sr^{-1}{\cdot}nm^{-1}}$ on the two new orbits compared to that of Aeolus under cloud-free skies

5. For the simulations, the Aeolus instrument parameters have been taken by the authors from the Algorithm Theoretical Basis Document (ATBD; Reitebuch et al., 2006). There is however a newer version of this document (issue 4.4, 20.04.2018), e.g. available by ESA for Aeolus CalVal users. Furthermore, the authors considered observations consisting of 50 accumulations (measurements) of 14 shots, resulting in a horizontal resolution of about 100.8 km per observation. However, Aeolus has 30 measurements per observation with 20 laser pulses per measurement (in the level 1B processing), resulting in a horizontal averaging length of about 90 km per observation. So the averaged wind observation uncertainties, derived by the authors in the present study, are only some estimates. It is proposed to use the newer/current parameters in future simulations in order to increase their usefulness

Response: Thanks to your suggestions. Considering that the difference in simulated wind observation uncertainties is large using new and old instrument parameters as shown in Fig. 3 in the reply to Reviewer 1, the new parameters were used in the simulation system in the revised manuscript. In addition, in the modified manuscript, one observation consists of 30 measurements with 20 laser pulses per measurement.

6. Eq. (7) has been numerically verified in the Appendix by neglecting noise (see item (5) in line 436). Consequently, Eq. (8) holds only for this restriction. Then, Eq. (8) is reformulated to Eq. (10) by using Eq. (6). However, Eq. (6) does contain noise, and consequently also Eq. (10) and its solution (11), which are used in the following investigations. The authors should comment on this. It becomes also not clear whether the results in Fig. (A3) have been obtained with or without noise.

Response: Thanks very much to your reminder. In original manuscript, the noise was not taken into account in the simulation system. In the modified manuscript, the noise was considered. The reason was explained in the Appendix.

Original: ln. 436 P17

The values of $\sigma_{R_{ATM}}$ and SNR_{Ray} are obtained using Eqs. (3), (4), and (6). In this study, the value of N_{noise} is assumed to be zero, which means the dark current of the detectors on Rayleigh channel is negligible.

Modified:

The values of $\sigma_{R_{ATM}}$ and SNR_{Ray} are obtained using Eqs. (3), (4), and (6). In addition, according to ADM-Aeolus ATBD Level1B products (Reitebuch *et al.*, 2018), the noise of detection chain for each measurement is 4.7 e^-/pixel. And 30 measurements are include in one observation, therefore, $C = 2N_{noise}^2 = 2 \times (4.7 \times 30)^2 = 39762$ in Eq. (10) which cannot be negligible.

7. In the discussion of Fig. 5 on pages 12-13, the authors should comment on the jump in the required laser pulse energy when going from the troposphere to the stratosphere. It is obviously due to the increase of the bin thickness and the resulting larger Rayleigh channel signals. Furthermore the authors should speculate why less energy is required in PBL, compared to the upper troposphere, though the PBL bin thicknesses are smaller, the laser energy and the Rayleigh channel backscattering damping are larger, and ESA's accuracy requirements are more restrictive in PBL. Is there any cross talk from the Mie channel caused by PBL aerosols?

Response (1): Thanks for your kind reminder, we will explain the jump when going from troposphere to stratosphere in line 321 of Page 12.

Original text: ln 320, Page 12

Higher energy is needed mostly in the upper level of troposphere and stratosphere near the regions close to Antarctic and Arctic circles. The closer the orbital LTAN is to noon, the averaged values of the required laser energy will become larger.

Modified:

Higher energy is needed mostly in the upper level of troposphere and stratosphere near the regions close to Antarctic and Arctic circles. On the boundary line with a height of 16 km, there is an obvious sudden jump in required laser energy, and the required laser energy is reduced. This is mainly because the vertical thickness of measurement bins changes from 1km to 2km at 16km, which makes the integration time of detection units of Rayleigh channel double. And larger atmospheric backscattered signal would be received. On the other hand, the required wind observation uncertainty increase from 2 m/s to 3 m/s in the stratosphere. Therefore, the required laser energy reduced suddenly when going from troposphere to stratosphere. The comparisons among the required laser energy of the three orbit illustrate that the closer the orbital LTAN is to noon, the averaged values of the required laser energy will become larger.

Response (2): Solar background noise has main impact on the wind observation uncertainties on Rayleigh channel. The impact of SBR on Mie channel is negligible (Rennie, 2017). Due to the widespread presence of aerosols in PBL, Mie channel is used to observe the wind in PBL. And the main topic of the manuscript is to study the impact of SBR on the Rayleigh channel wind observations. Therefore, the Rayleigh wind observations in PBL is not considered. Sentences in the original text may misunderstand readers, we will modify as follows:

Original: ln 279, Page 10

In fact, the Mie channel is mostly used for wind observations in the PBL, which are of higher accuracy. It is meaningless to study the wind observation accuracy of the Rayleigh channel in the PBL, the accuracy of the Rayleigh channel in the PBL is not considered in the following of this paper.

Modified:

In fact, the Mie channel is mostly used for wind observations due to the widespread presence of aerosols in PBL. Therefore, the accuracy of the Rayleigh channel in the PBL is not considered in the following of this paper.

As to the questions why less energy is required in PBL, in the PBL, the Mie channel wind observation uncertainties is much less than that of Rayleigh channel as Fig. 6 (a) shown. However, the photon counts of Mie channel excited by atmosphere aerosols and solar background radiation is also much less than that of Rayleigh channel as Fig. 6 (b, c) shown. The optical properties of aerosols are obtained from RMA dataset. So I don't know the reasons for the phenomenon that the wind observation accuracy on Mie channel is higher than that of Rayleigh channel. It may be due to the detection mechanism of Mie channel. Hope for further discussions to the question with reviewers.

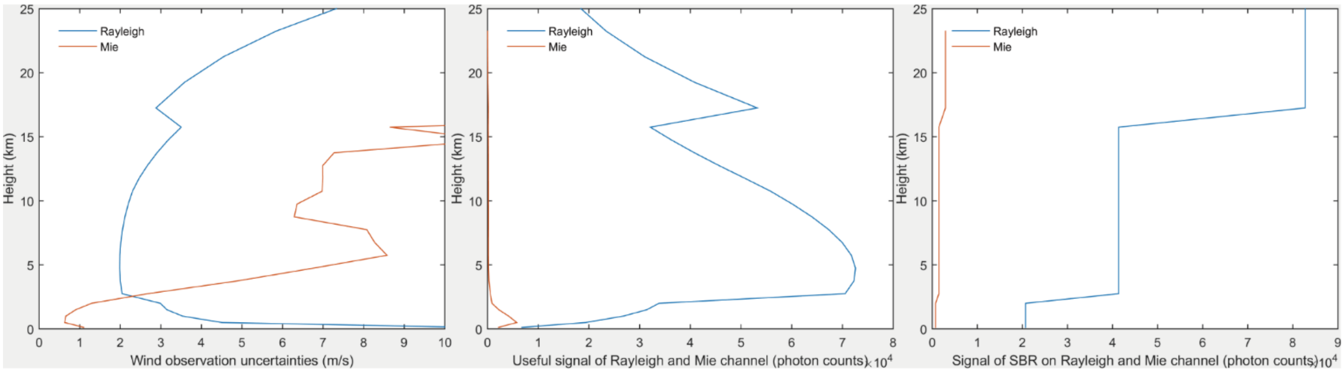

Fig. 6. Comparisons between the wind observations of Rayleigh channel and Mie channel. (a) Wind observation uncertainties; (b)useful signal of atmospheric backscatter; (c)signal excited by solar background.

minor specific comments

8. The authors should be more specific in the abstract in line 15 by writing "increment of averaged Rayleigh channel wind observation uncertainties", since they consider only Rayleigh channel winds.

Response: Done.

9. The authors write in lines 108-109: "Figure 1(b) shows that the solar zenith angle of the observation points of the two new Aeolus-type instruments is low compared to that of Aeolus, and thus lead to larger SBR." However, this figure does not show solar zenith angles. The authors should comment on this.

Response: Thanks for your reminder. From Fig. 1(b), we cannot get the information that the solar zenith angle of two new Aeolus-type instruments is low compared to that of Aeolus. On the other hand, the sentence is not useful for the meaning of Section 2.1, so it has been deleted in the revised manuscript

10. In lines 273-274: Where do the 18 wind uncertainty profiles come from? And is there 1 profile for every 10° latitude stripe?

Response: Yes, there is 1 profile for every 10◦ latitude stripe.

In Fig. 2 of the manuscript (Fig. 3 of modified manuscript), the maximum SBR of each grid (the earth was divided into 1◦×1◦ grids) was illustrated. Because the SBR is not much different at the same latitude as Fig. 2 of the manuscript shows, the SBR are averaged within 10◦ latitude. Then the 10◦ latitude averaged atmospheric conditions were obtained from Ozone

Monitoring Instrument (OMI) database as mentioned in subsection 2.2 of the manuscript. Finally, the 10◦ latitude averaged uncertainties of wind observation on Rayleigh channel derived and show in Fig. 3 of the manuscript.

11. Table 2 shows that the averaged increment in the wind observation uncertainties of the 12:00 orbit in the stratosphere is 1.23 m/s, compared to the 18:00 Aeolus orbit. In the text however, 1.4 m/s is reported (lines 16, 286, and 380). Thus the value in the text could be lowered.

Response: In the manuscript, due to the instrument parameters are changed in simulation system, and noise was considered. The results were changed. Furthermore, Table 2 of original manuscript was removed.

12. the authors should rename the title of Section 4.4 to "Uncertainties of wind observations resulting from an increased laser pulse energy" because they only consider an increased laser pulse energy as a new instrument parameter. Furthermore, the authors should mentioned in line 341 that their proposed laser energy of 80 mJ has been already required by ESA (see e.g. ATBD; Reitebuch et al., 2018). Moreover, the authors should delete the phrase "new instrument parameters, of which" in the caption of Fig. 6. Additionally, the authors should replace "instrument parameters" by "laser energies" in the caption of Tab. 6.

Response (1): Done, title of Section 4.4 was renamed.

Original:

4.4 Uncertainties of wind observations based on new instrument parameter proposal

Modified:

4.4 Uncertainties of wind observations resulting from an increased laser pulse energy

Response (2): Done.

Original: ln. 341, P13

Considering the accuracy requirements of ESA and accuracy level of Aeolus, while taking the existing technical level into account, the laser energy of the two new spaceborne DWLs is set to 80 mJ.

Modified:

Considering the accuracy requirements of ESA and accuracy level of Aeolus, while taking the existing technical level into account, the laser energy of the two new spaceborne DWLs is set to 70 mJ in this paper. In fact, the laser energy of 80 mJ has been already required by ESA in ATBD (Reitebuch et al., 2018).

Response (3): Done.

Original: ln 353, P14

Figure 6. *The zonal distributions of wind observation uncertainties of the three spaceborne DWLs with new instrument parameters, of which the laser energy of Aeolus is 60 mJ, and the laser energy of the two new Aeolus-type spaceborne DWLs is 80 mJ.*

Modified:

Figure 8. The zonal distributions of wind observation uncertainties of the three spaceborne DWLs with the laser energy of Aeolus is 60 mJ, and the laser energy of the two new Aeolus-type spaceborne DWLs is 70 mJ.

Response (4): Tab. 6 of original manuscript was removed.

13. In the abstract, the authors should recall the conditions for which they have derived their results (no clouds, aerosols, noise (?), laser energies of 60 mJ and 80 mJ respectively, number of measurements per observation, number of laser shots per measurement, only Rayleigh channel winds)

Response: Done.

The following changes are proposed to improve the readability of the paper.

14. There are several incidences where different statements are separated only by a comma in one sentence (e.g. lines 10-13). Please check the paper for that and introduce separate sentences.

Response: Thanks for your suggestions. We made corresponding modifications in the revision.

15. Please replace "by 0.18, 0.69 m/s" by "by 0.18 and 0.69 m/s" in line 62.

Response: the sentence was removed in the revision.

16. Please provide the reference for the quantum efficiency of the Rayleigh channel detector in line 181 (obviously Reitebuch et al., 2006).

Response: Done

Original: ln 181, P7

E_Q and E_O denote the quantum efficiency of the detector on Rayleigh channel.

Modified:

E_Q and E_O denote the quantum efficiency of the detector on Rayleigh channel (Reitebuch *et al.*, 2018)

17. In the caption of Fig. 2, please interchange the 2. and 3. sentence (i.e. first the 3. and then the 2. sentence as the last sentence). Furthermore, do Figs. (c,d) and (e,f) really show numerical differences to Figs. (a,b)? Or do the contours in Figs. (c,d) and (e,f) only show values from the right-hand side scale?

Response: Thanks for your suggestions. The 2. and 3. sentence of the caption of Fig. 2 (Fig. 3 of modified manuscript) were interchanged.

Fig. (c, d) and (e, f) did show numerical differences to Figs. (a, b).

18. Please add the SBR increments [$mW*m^{-2}*sr^{-1}*nm^{-1}$] 60.68-20.99=39.69 and 76.36-20.99=55.37 in line 263 because they are listed in the abstract and in the summary.

Response: Done.

Original: ln 263, P10

Statistics illustrate that the averaged SBR of the three spaceborne DWLs are 20.99, 60.68, and 76.36 $mW{\cdot}m^{-2}{\cdot}sr^{-1}{\cdot}nm^{-1}$ *respectively.*

Modified:

Statistics illustrate that the averaged SBR illustrated in Fig. 3 are 20.99, 60.68, and 76.36 $mW{\cdot}m^{-2}{\cdot}sr^{-1}{\cdot}nm^{-1}$ respectively near the summer and winter solstice periods. The averaged increments of SBR received by new spaceborne DWLs are 60.68-20.99=39.69 $mW{\cdot}m^{-2}{\cdot}sr^{-1}{\cdot}nm^{-1}$ and 76.36-20.99=55.37 $mW{\cdot}m^{-2}{\cdot}sr^{-1}{\cdot}nm^{-1}$ compared to that of Aeolus.

19. The sentence in lines 263-264 ("The quantile statistics of SBR is presented in Table 1, which means that the corresponding percentages of the grids (the earth is divided into 1°×1° grid) of which the SBR will be smaller than the values listed in the first line of Table 1.") is unclear. Please provide a clearer formulation, e.g. also by adding an example (e.g., 90% of the grid points (?) or tiles (?) of the 12:00 orbit have SBR values smaller than 105.77 $mW*m^{-2}*sr^{-1}*nm^{-1}$).

Response: In the revision, Table 1 was removed, for which may be a bit redundant. The similar expression appeared in Table 3 (Table 1 of modified manuscript). We added an example to make it clear.

Original: ln 311, P12

The quantiles of the required energy of the two spaceborne DWLs are shown in Table 3 which means that the corresponding percentages of the bins whose accuracy will reach the accuracy level of Aeolus once the laser pulse energy equals to the specific values.

Modified:

The quantiles of the required energy of the two spaceborne DWLs are shown in Table 1, which means that the corresponding percentages of the bins whose accuracy will reach the accuracy level of Aeolus once the laser pulse energies equal to the specific values. For example, 90% of the bins will reach or exceed the accuracy level of Aeolus when the laser energy is 70.37 mJ for the spaceborne DWL operating on the 15:00 orbit.

20. Please replace "upper layer of troposphere and stratosphere" by "upper layer of atmosphere" in lines 277-278.

Response: Thanks for your suggestions.

Because in the lower layer of stratosphere, the wind observation uncertainties would meet the accuracy requirement of ESA. So we think the original expression is more accurate.

21. In the captions of Figs. 3, 5, and 6, the authors write that the "correspondence relationship between the subgraphs and orbits, seasons is consistent with Fig. 2". It is proposed to reformulate this sentence, e.g. to "The arrangement of the subgraphs corresponds to that of Fig. 2".

Response: Done. Thanks for your suggestions.

22. In lines 298-299: Is the accuracy level of Aeolus, mentioned here, that one shown in Figs. 3 (a) and (b)? If so, please note this here.

Response: Yes, the accuracy level of Aeolus is the one shown in Figs. 3(a) and (b). The expression was added in the revision.

Original: ln 298, P11

Supposed that the wind observation accuracy of the two new spaceborne DWLs is required to reach the accuracy level of Aeolus, which can be used for joint observations of the three satellites.

Modified:

Supposed that the wind observation accuracy of the two new spaceborne DWLs is required to reach the accuracy level of Aeolus as shown in Figs. 5(a, b), which can be used for joint observations of the three satellites

23. It is assumed that the results shown in Figs. 6 (a) and (b) are identical to those of Figs. 3 (a) and (b). It is however not directly seen due to the different color scales. If so, please make a corresponding note in the text or caption of Fig. 6. If not, please explain why it is not the case.

Response: Thanks for your suggestions.

Figs. 6 (a, b) are identical to those of Figs. 3 (a, b). Because both of the laser energies are 60 mJ. We will make a corresponding note in the text in the revision.

Original text: ln 365 P15

The comparison between Fig. 6(c-f) and Fig. 3(c-f) illustrate that, as for the two new spaceborne DWLs, when the laser energy increases from 60 mJ to 80 mJ, the observation accuracy would be improved significantly.

Modified:

The wind observation uncertainty distributions of the three spaceborne DWLs are derived as is shown in Fig. 8. Note that Figs. 8(a, b) are identical to those of Figs. 5 (a, b), for that both of them are obtained with laser energies of 60 mJ.

24. technical corrections

lines 53-55: Doppler wind lidar which sensing -> senses, Mie/Rayleigh channel sensing

-> senses

line 122: expect the mean altitude -> except

Different notations are used for the uncertainty of wind observation in the Rayleigh channel in Eqs. (1) and (8). Please use a consistent notation.

line 233: the wind observation uncertainty which were calculated -> was

line 454: is also need -> needed

line 463: Subsect. 3.4 does not exist, replace by Subsect. 3.3

Response: We're very sorry for the low-level mistakes. And we will correct these mistakes in the revised manuscript.

References:

Reitebuch, O., Huber, D. and Nikolaus, I.: ADM-Aeolus ATBD Level 1B Product, European Space Agency, 2018.